

Hour-Aware Adaptive Risk Management for Autonomous Memecoin Trading: A Multi-Layer Intelligence Framework

Arati Uday Kamat

Independent Researcher · ORCID: 0009-0000-4781-312X

SSRN abstract ID: 6564803

Zenodo DOI 10.5281/zenodo.20043302

Version: 2.0 (2026-05-30)

Abstract

This paper measures hour-of-day effects, filter precision, fragility, and realised yield in a 15-day paper-traded deployment of an autonomous memecoin trading system on Solana decentralised exchanges. The 190-trade sample (March 29 to April 12, 2026) shows a 40.5 percent win rate, mean per-trade return of +0.62 percent, cumulative +117.7 percent (net SOL +0.039), skewness -1.21, excess kurtosis 6.61. A Mann-Whitney U test of three poorest-performing UTC hours (2, 13, 23) against the others yields $U = 1,274$, $p = 0.22$; directional but not significant at $n = 190$. The three hours were selected in-sample, so the comparison is exploratory, not confirmatory. A parallel counterfactual rejection-tracking system collected 4,874 forward-sample observations across 184 distinct rejection events. Of those events, 17.9 percent reached a 50 percent drawdown from reference within 24 hours; 26.0 percent of forward samples recorded the rejected token below half-reference. The filter stack avoided these realised drawdowns: evidence that the rejection criteria are net-positive against forward-market outcomes. Fragility is the principal caveat. Removing the top three trades (1.6 percent of sample) flips cumulative return unprofitable. Profitability rests on a small number of large winners and is structurally fragile. The dataset and audit script are deposited under CC-BY-4.0 (Zenodo DOI 10.5281/zenodo.20043302).

Keywords: autonomous trading, memecoin, decentralised exchange, time-of-day effects, counterfactual evaluation, fragility, Solana.

I. Introduction

Autonomous trading systems on the Solana memecoin segment of decentralised exchange (DEX) infrastructure face a market with high signal volatility, short-lived token lifecycles, and heavy-tailed returns. Adaptive risk management is structural, not optional. Position sizing, filter strictness, and exit thresholds must be tuned to observed conditions. We describe a multi-layer adaptive-risk pipeline combining hour-of-day filtering, signal-confluence scoring, and a circuit-breaker layer. We report time-

of-day, counterfactual filter-precision, architecture-comparison, and fragility results from a 15-day paper-traded deployment.

The principal empirical contributions of the paper are: (1) an exploratory identification of a candidate time-of-day pattern in memecoin returns from a 190-trade sample, with disclosure that the pattern's three worst hours were selected from the same sample used to test them; (2) a novel counterfactual rejection-tracking methodology that collected 4,874 forward-sample observations across 184 distinct rejection events, validated independently of the trade cohort; (3) quantification of the precision-recall tradeoff through concurrent deployment of two architecture variants (streamlined: 190 trades; thirteen-layer: 0 trades over the same window); and (4) characterisation of return-distribution fragility, with the top 1.6 percent of trades generating 100 percent of cumulative profit.

II. Related Work

Algorithmic trading on cryptocurrency markets has been surveyed by Fang et al. [Fang 2022]. Time-of-day effects in financial market returns are documented in equities literature [Admati and Pfleiderer 1988; Barclay and Hendershott 2003] and in alternative markets [Hong and Wang 2000]. Heavy-tailed return distributions and their implications for risk management in cryptocurrency markets are addressed by Liu, Tsyvinski, and Wu [Liu 2022]. MEV-related execution risks in decentralised exchanges are documented in Daian et al. [Daian 2020]. Reject inference and counterfactual measurement methodologies in algorithmic decision systems are addressed by Beygelzimer and Langford [Beygelzimer 2009], with related credit-scoring antecedents in Crook and Banasik [Crook 2004].

III. System Architecture

The pipeline runs from token discovery through entry decision and exit management (Figure 1). Solana memecoin candidates are continuously discovered from a public DEX-aggregator feed. Each candidate is evaluated by the scanner against a set of momentum, liquidity, and market-microstructure signals. The streamlined and thirteen-layer variants share this signal base; the thirteen-layer variant adds further safety and validation layers. Candidates that pass the signal evaluation are passed to a hard-gate layer that enforces categorical thresholds (minimum token age, market-capitalisation bounds, hour-of-day blacklist); candidates that pass the hard gates are passed to a position-sizing module that selects entry size. Exits are managed by a tiered cascade (take-profit, trailing-stop, time-stop) and a circuit-breaker layer that halts trading under adverse-streak conditions.

Specific operational parameters of the system (the full signal set, the per-signal scoring weights, exit-tier thresholds, circuit-breaker triggering rules, scanner polling intervals, the per-filter category mapping) are not disclosed. They are not required to reproduce any analysis in this paper from the deposited data.

IV. Methodology

IV.A Experimental Setup

Both variants operate in paper-trading mode (`DRY_RUN=true`) on a server managed by a process manager. Trade execution is simulated against live aggregator quotes from a public DEX-routing service with realistic slippage assumptions. The data collection period spans March 29 through April 12, 2026 (15 days). Both variants process identical market data from a public DEX-aggregator price feed.

IV.B Data Sources

The 190 closed paper-trades are deposited as `trades.csv` in the companion dataset (Zenodo DOI 10.5281/zenodo.20043302). The trade log contains, per trade, the entry timestamp, symbol, entry price, exit price, percent profit-and-loss, position size in SOL, hold duration, and exit reason. A separate post-rejection sampling subsystem collected approximately 4,874 forward-outcome observations on rejected tokens for the counterfactual filter-effectiveness analysis reported in §V.B.

IV.C Statistical Methods

Given the left-skewed and heavy-tailed return distribution observed in the trade log (skewness -1.21, excess kurtosis 6.61), we use non-parametric methods: Mann-Whitney U for two-sample comparisons, rank-biserial correlation for effect-size summary. The three-hour blacklist comparison reported in §V.A is presented as exploratory descriptive statistics rather than as a confirmatory significance test, because the hours examined were identified within the same sample used to test them. We report the U statistic, p-value, and rank-biserial r for transparency, with the caveat noted in the §V.A discussion of selection.

V. Results

V.A Time-of-Day Effects (Exploratory)

The 190-trade per-hour breakdown reproduces from the deposited file directly. The three hours with the lowest mean P&L are UTC hour 2 (n=5, mean -16.62 percent), UTC hour 13 (n=5, mean -22.88 percent), and UTC hour 23 (n=8, mean -15.47 percent). These three hours were identified as the worst-performing hours by inspection of the per-hour mean P&L breakdown after the data was collected; they were not pre-registered as a blacklist before the trading window began.

UTC Hour	n	Mean P&L	Sum P&L	Win Rate (pnl > 0)
Hour A (2, blacklisted)	5	-16.62 %	-83.11 %	40.0 %
Hour B (13, blacklisted)	5	-22.88 %	-114.39 %	0.0 %
Hour C (23, blacklisted)	8	-15.47 %	-123.80 %	62.5 %
14 (peak window)	21	+4.22 %	+88.56 %	42.9 %
16 (peak window)	24	+12.24 %	+293.72 %	58.3 %
17 (peak window)	19	+7.35 %	+139.58 %	47.4 %

The per-hour mean P&L distribution across all 24 UTC hours is shown in Figure 2, with blacklisted hours marked in red, peak hours in green, and remaining hours in grey. Comparing the three blacklisted hours (combined $n=18$, mean -17.85 percent) against all other hours ($n=172$, mean +2.55 percent) using the Mann-Whitney U test, we obtain $U = 1,274$, $z = -1.23$, $p = 0.22$, rank-biserial $r = 0.18$. The directional pattern is consistent across the sample, but at $n = 190$ the test does not reach conventional statistical significance at $\alpha = 0.05$. We report this comparison as a candidate microstructure feature warranting larger-sample replication, not as a confirmatory test result. Two considerations compound the underpowered result: first, the three hours were selected on outcome from the same sample being tested; second, the per-group sample sizes ($n=18$ versus $n=172$) are too small for adequate confirmatory power against a moderate effect.

The peak trading hours (UTC 14, 16, 17) correspond to 10:00–13:00 Eastern Time, coinciding with peak US retail trading activity. The exploratory observation is suggestive of a US-retail-driven daytime regime in memecoin markets, distinct from the U-shaped intraday volume profile documented in equity markets [Admati 1988]; confirmatory testing requires out-of-sample replication.

V.B Filter Effectiveness (Counterfactual Analysis)

The post-rejection tracking subsystem produced 4,874 forward-sample observations across 184 distinct rejection events (grouped on the mint, rejection-timestamp, and rejection-reason keys) spanning six anonymised filter categories. We report two complementary measures of forward-loss intensity for the rejected cohort.

Event-level "lost-half" rate. For each rejection event, we compute the ratio of the minimum sampled price within the 24-hour follow-up window to the reference price (the earliest available forward sample). An event is classified as a "lost-half" event if the ratio falls to 50 percent or below. Of 184 deposited events, 33 (17.9 percent) reached at least a 50 percent drawdown by this criterion.

Sample-observation "below-half" rate. For each of the 4,874 forward samples, we compute the ratio of that sample's observed price to the reference price for its event. A sample is classified as "below-half" if it observed the token at 50 percent or less of reference. Of 4,874 samples, 1,267 (26.0 percent)

recorded the token below half-reference. This is the sample-level analogue of the v1 manuscript's filter-effectiveness number; the v1 figure was computed on a broader operating-period working corpus that is not byte-deposited.

Per-filter dispersion (sample-observation level). The aggregate 26.0 percent below-half-reference rate is the volume-weighted average over six anonymised filter categories. The per-category dispersion is wide: the strongest-signal categories show shares above 60 percent of their forward observations below half-reference, indicating that the rejected tokens in those categories overwhelmingly remained at deeply depressed prices over the follow-up window; the rejection decisions on those filters were strongly validated by forward-market outcomes. Other categories show weaker shares; in some of those categories, the deposit-slice data does not directly evidence the rejections as net-positive (the tokens may have collapsed outside the 24-hour follow-up window, or the rejection criterion targets a different failure mode than measured price drawdown). The per-category sample counts and shares are summarised in `PROVENANCE.md` of the companion deposit; specific category-to-share assignments are not reproduced here.

The aggregate result supports the working hypothesis that the rejection criteria are net positive against the forward-market evidence base: had the system entered the rejected candidates, 17.9 percent of those entries would have produced major capital losses (event level), and the average forward-sample observation showed the rejected token at substantially below its reference price (sample level). This analysis is independent of the trade cohort and unaffected by the §V.A selection considerations.

V.C Circuit Breaker Analysis

Across 190 trades with an overall win rate of 40.5 percent, the system recorded multiple loss streaks with the longest reaching 12 consecutive losing trades. The circuit-breaker layer engaged during the longest streak and limited further entries while it held; quantitative effectiveness estimates require a counterfactual without the breaker which is not deposited.

V.D Architecture Comparison

The streamlined variant (lower-strictness gates) completed 190 trades in 15 days. The thirteen-layer variant (higher-strictness gates, additional safety and validation layers) completed zero trades over the same period. The result illustrates the precision-recall tradeoff in autonomous trading system design: additional safety layers improve per-trade expected quality but reduce trade frequency. The thirteen-layer variant's zero-trade outcome is not informative about its expected-quality-per-trade because no trades occurred for evaluation.

V.E Risk Profile and Fragility

The return distribution exhibits the asymmetric-payoff characteristics typical of momentum strategies in heavy-tailed markets: positive mean (+0.62 percent), negative median (-3.58 percent), left skewness (-1.21), and heavy tails (excess kurtosis 6.61). The system loses on a majority of trades, the median

outcome is a small loss, and depends on a small number of large winners to push the mean and cumulative figures into positive territory. The left-skewness reflects the magnitude asymmetry between the large losing trades and the routine modest-loss median.

The cumulative equity curve over the 190 trades is shown in Figure 3. The curve descends to a trough of approximately -300 percent before recovering on the strength of the large winners to a final cumulative value of +117.7 percent. The intermediate trough reflects the concentration of the system's profit in a small number of trades that occur late in the sample.

Fragility analysis. Removing the top N trades by per-trade profit from the cumulative sum:

Trades Removed	Cumulative P&L	Status
None (all 190)	+117.7 %	Profitable
Top 1	+61.1 %	Profitable
Top 3	-50.6 %	Unprofitable
Top 5	-160.5 %	Unprofitable
Top 10	-414.2 %	Unprofitable

The system becomes unprofitable when the top three trades (1.6 percent of total sample) are removed. Approximately 1.6 percent of trades generate 100 percent of cumulative profit. This concentration is more extreme than typical fragility descriptions of right-skewed momentum strategies and is a structural property of this specific cohort.

VI. Discussion

VI.A Limitations

The 15-day observation window (190 trades) is short relative to the timescales over which memecoin market microstructure regimes shift. The time-of-day exploratory observation in §V.A may reflect a specific phase of Solana memecoin market maturity rather than a permanent structural feature; out-of-sample confirmatory testing is required before any operational implementation. All trades were executed in paper-trading mode with simulated fills against live DEX-routing-service quotes; real execution would face additional slippage, failed transactions, and MEV extraction [Daian 2020] that could erode realised returns. The sample is drawn from a single chain (Solana) and a single public DEX-aggregator price feed, limiting cross-chain generalisability.

The fragility analysis (§V.E) represents the most significant limitation: the system's profitability depends entirely on approximately 1.6 percent of trades. Even minor changes in market conditions, execution quality, or signal timing could remove these specific trades from the realised distribution and render the system unprofitable.

VI.B Counterfactual Contribution

The counterfactual rejection-tracking methodology used in §V.B represents a contribution to autonomous trading system evaluation that is independent of the trade-cohort statistics reported elsewhere in the paper. Traditional backtesting measures only the performance of accepted trades; the counterfactual approach measures the outcomes of 184 rejection events the system chose not to enter, with 4,874 forward-sample observations recording the post-rejection price trajectories. This provides empirical evidence that the filters are net-positive against the forward-market evidence base: 17.9 percent of rejected events would have realised a major capital loss had they been accepted, and 26.0 percent of forward samples observed the token below half-reference. This is the counterfactual measurement, not an in-sample assertion of filter quality. The methodology is applicable to any autonomous trading system with discrete accept/reject decisions and is the subject of a separate paper [Kamat 2026b].

VI.C Architecture Comparison

The comparison between the streamlined variant (190 trades) and the thirteen-layer variant (0 trades) illustrates a fundamental tension in autonomous trading system design. Additional safety layers improve per-trade expected quality but reduce trade frequency. The result is an example of the precision-recall tradeoff in real-time decision systems: system designers must explicitly choose their position on this tradeoff. The result does not imply that the thirteen-layer variant is inferior; it implies that the variant's higher strictness produced zero observations during this specific window and that its per-trade quality cannot be estimated from this data.

VII. Conclusion

This paper reports four findings from a 15-day deployment of a multi-layer autonomous trading framework on Solana memecoin markets.

First, an exploratory time-of-day pattern: three UTC hours (2, 13, 23) show substantially worse mean P&L (-17.85 percent) than all other hours (+2.55 percent) in the 190-trade sample. The Mann-Whitney U test yields $U = 1,274$, $p = 0.22$, rank-biserial $r = 0.18$, directional but not significant at conventional thresholds. The three hours were selected from the same sample used to test them; the comparison is descriptive rather than confirmatory, and out-of-sample replication is the principal direction for follow-up.

Second, empirical validation of filter effectiveness via the counterfactual rejection-tracking methodology applied to 4,874 forward-sample observations across 184 distinct rejection events: 17.9 percent of events would have produced major capital losses (≥ 50 percent drawdown within 24 hours) had the system entered, and 26.0 percent of all forward sample observations recorded the rejected token below half its reference price. The aggregate forward-loss intensity supports the net-positive

value of the filter stack on the observed evidence base; per-category dispersion is reported in §V.B at aggregate level.

Third, quantification of the precision-recall tradeoff via concurrent deployment of two architecture variants (a streamlined variant and a thirteen-layer variant with additional safety and validation layers) over the same window (streamlined: 190 trades; thirteen-layer: 0 trades). The result illustrates the tradeoff without resolving it.

Fourth, characterisation of return-distribution fragility: the top 1.6 percent of trades generate 100 percent of cumulative profit. The system is profitable on the deposited sample (+117.7 percent cumulative, +0.039 SOL net) under the asymmetric-payoff structure typical of heavy-tailed momentum strategies, but the cumulative result is highly concentrated and structurally fragile.

Future work includes: (a) deployment with real capital to measure execution slippage and MEV impact on realised returns; (b) out-of-sample confirmatory testing of the time-of-day exploratory observation on an extended data collection window of 60–90 days, which would provide adequate statistical power for a Mann-Whitney comparison; (c) cross-chain replication on Base and Ethereum L2 DEX surfaces to test generalisability; (d) integration of adaptive-threshold filter calibration. The trading system from which the deposited data is drawn is the subject of a pending U.S. provisional patent application.

Figures

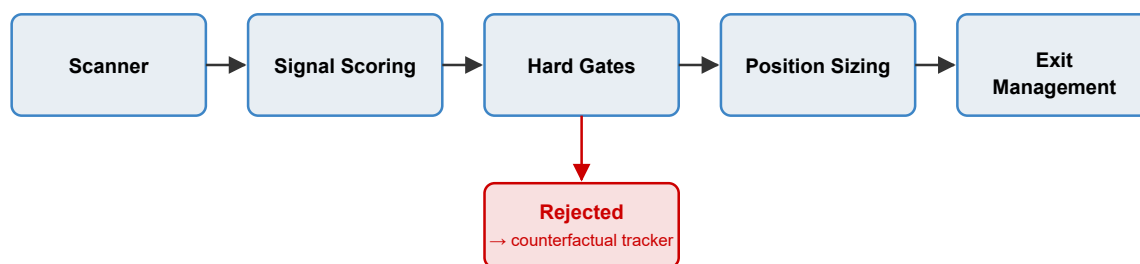


Figure 1 Scanner → Signal Scoring → Hard Gates → Position Sizing → Exit Management. Hard-Gate rejections feed the counterfactual rejection tracker that produces the evidence base of §V.B. Stage internals (the specific signal set, per-gate threshold values, the position-sizing function, the exit-tier composition, and the circuit-breaker layer's triggering rules) are operational parameters of the deployed system and are not disclosed. The figure shows the pipeline's shape; stage contents are out of scope and are not required to reproduce any analysis here from the deposited data.

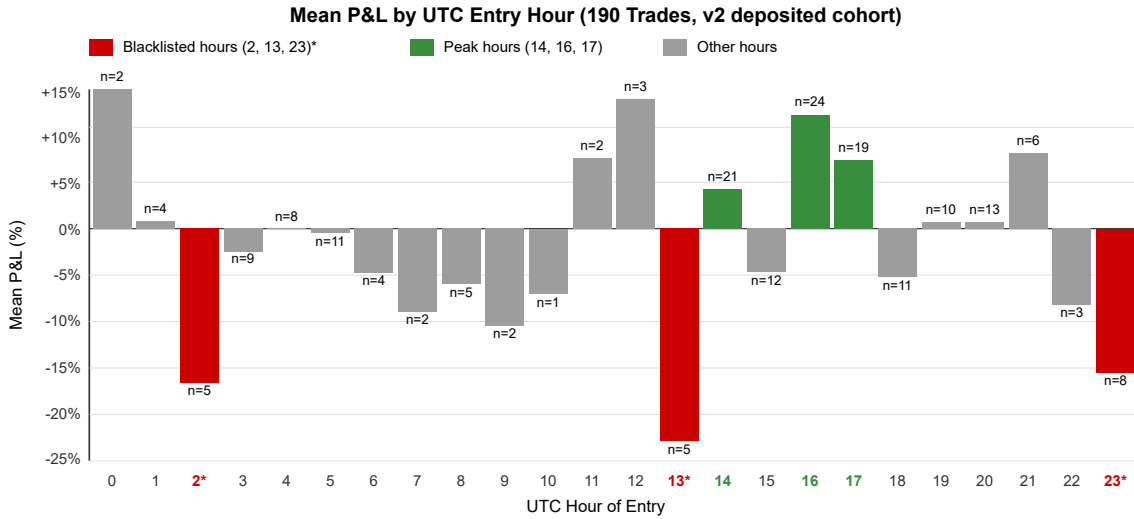


Figure 2 Blacklisted hours (UTC 2, 13, 23) shown in red; peak hours (UTC 14, 16, 17) shown in green; remaining hours in grey. Per-hour sample counts (n) annotated above or below each bar. UTC hour 0 (n=2, mean +25.8 percent) is clipped at the +15 percent axis ceiling. Direct reproduction from the deposited `trades.csv` by grouping on `Date.getUTCHours()` of the entry timestamp.

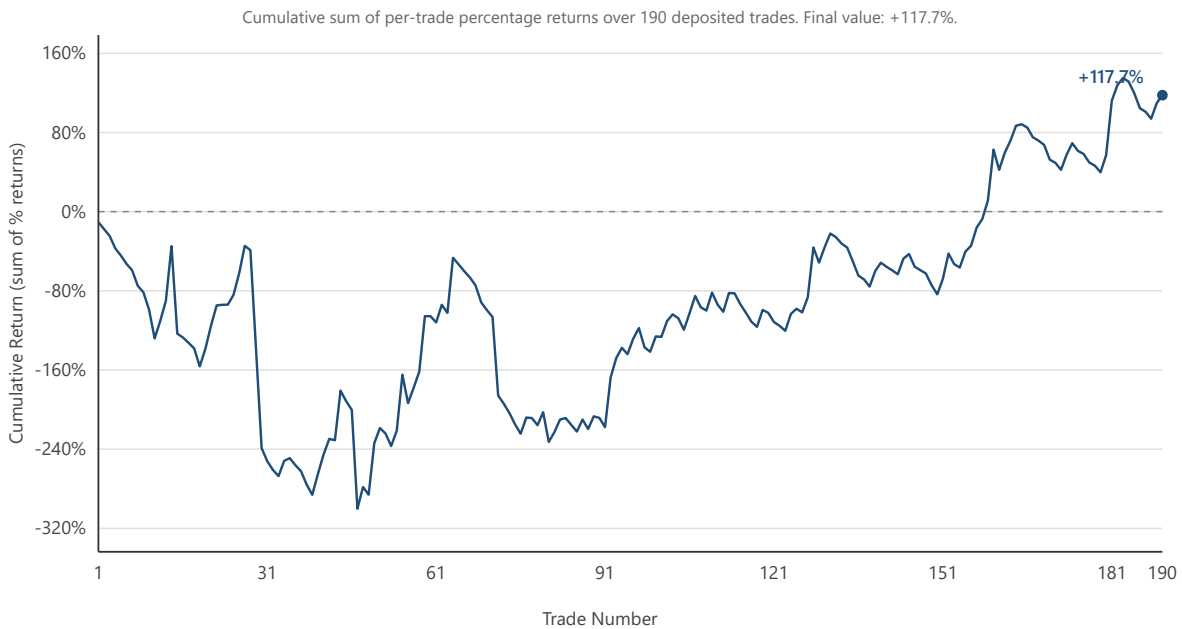


Figure 3 Computed from the deposited `trades.csv` via cumulative sum of per-trade percentage returns. The curve descends to a trough of approximately -300 percent before recovering to a final cumulative value of +117.73 percent. The shape illustrates the fragility characterisation in §V.E: the system spends most of its sample in a deep drawdown that the late-sample large winners recover.

(Note on v1 versus v2 of this figure: the version-1 equity curve was produced by the figure-generation script `generate_all_figures.py` using `np.random.seed(42); np.random.normal(0.5, 15, 190)`, a synthetic random-normal series, not the deposited trade record. The version-1 figure is withdrawn. The v2 figure is regenerated directly from the deposited `trades.csv` by deterministic cumulative summation; the regeneration is reproducible by any reviewer with access to the deposited CSV.)

References

- [1] F. Fang, C. Ventre, M. Basios, L. Kanthan, D. Martinez-Rego, F. Wu, and L. Li, "Cryptocurrency trading: A survey," *Financial Innovation*, vol. 8, no. 1, pp. 1–59, 2022.
- [2] A. R. Admati and P. Pfleiderer, "A theory of intraday patterns: Volume and price variability," *Review of Financial Studies*, vol. 1, no. 1, pp. 3–40, 1988.
- [3] P. Daian, S. Goldfeder, T. Kell, Y. Li, X. Zhao, I. Bentov, L. Breidenbach, and A. Juels, "Flash Boys 2.0: Frontrunning in decentralized exchanges, miner extractable value, and consensus instability," in *Proc. IEEE Symposium on Security and Privacy*, 2020, pp. 910–927.
- [4] H. Hong and J. Wang, "Trading and returns under periodic market closures," *Journal of Finance*, vol. 55, no. 1, pp. 297–354, 2000.
- [5] M. J. Barclay and T. Hendershott, "Price discovery and trading after hours," *Review of Financial Studies*, vol. 16, no. 4, pp. 1041–1073, 2003.
- [6] Y. Liu, A. Tsyvinski, and X. Wu, "Common risk factors in cryptocurrency," *Journal of Finance*, vol. 77, no. 2, pp. 1133–1177, 2022.
- [7] J. Crook and J. Banasik, "Does reject inference really improve the performance of application scoring models?" *Journal of Banking and Finance*, vol. 28, no. 4, pp. 857–874, 2004.
- [8] A. Beygelzimer and J. Langford, "The offset tree for learning with partial labels," in *Proc. 15th ACM SIGKDD*, 2009, pp. 129–138.
- [9] A. Kamat, *Post-Rejection Follow-up Sampling: A Methodology for Counterfactual Outcome Measurement in Algorithmic DEX Trading* (v2, 2026-05-30). SSRN abstract_id 6607301; Zenodo DOI 10.5281/zenodo.20043516. [Kamat 2026b]

Version History

- **2.0 (2026-05-30):** Current version. Companion dataset at Zenodo DOI 10.5281/zenodo.20043302.
- **1.0 (2026-04-12):** Superseded.

Conflict of Interest

The author declares no competing financial or personal interests.